The antibody zalutumumab inhibits epidermal growth factor receptor signaling by limiting intra- and intermolecular flexibility

Jeroen J. Lammerts van Bueren*, Wim K. Bleeker*, Annika Brännström†, Anne von Euler†, Magnus Jansson†, Matthias Peipp‡, Tanja Schneider-Merck‡, Thomas Valerius‡, Jan G. J. van de Winkel*§, and Paul W. H. I. Parren*¶

*Genmab, 3508 AD, Utrecht, The Netherlands; †Sidec, SE-164 40 Kista, Sweden; ‡Division of Nephrology and Hypertension, Christian-Albrecht-University, 24105 Kiel, Germany; and §Immunotherapy Laboratory, Department of Immunology, University Medical Centre Utrecht, 3584 EA, Utrecht, The Netherlands

Edited by Michael Sela, Weizmann Institute of Science, Rehovot, Israel, and approved February 7, 2008 (received for review October 8, 2007)

The epidermal growth factor receptor (EGFR) activates cellular pathways controlling cell proliferation, differentiation, migration, and survival. It thus represents a valid therapeutic target for treating solid cancers. Here, we used an electron microscopy-based technique (Protein Tomography) to study the structural rearrangement accompanying activation and inhibition of native, individual, EGFR molecules. Reconstructed tomograms (3D density maps) showed a level of detail that allowed individual domains to be discerned. Monomeric, resting EGFR ectodomains demonstrated large flexibility, and a number of distinct conformations were observed. In contrast, ligand-activated EGFR complexes were detected only as receptor dimers with ring-like conformations. Zalutumumab, a therapeutic inhibitory EGFR antibody directed against domain III, locked EGFR molecules into a very compact, inactive conformation. Biochemical analyses showed bivalent binding of zalutumumab to provide potent inhibition of EGFR signaling. The structure of EGFR–zalutumumab complexes on the cell surface visualized by Protein Tomography indicates that the cross-linking spatially separates the EGFR molecules' intracellular kinase domains to an extent that appears incompatible with the induction of signaling. These insights into the mechanisms of action of receptor inhibition may also apply to other cell-surface tyrosine kinase receptors of the ErbB family.

EGFR | mechanism of action | protein tomography

Epidermal growth factor receptor (EGFR) is a 180-kDa glycoprotein receptor tyrosine kinase of the ErbB family (1). The receptor has several ligands with similar structures of which EGF and TGF-α are the most studied. Signaling via EGFR enhances processes responsible for cell growth and differentiation, including promotion of proliferation, angiogenesis, cell migration, and inhibition of apoptosis. Activation of this growth factor receptor is tightly regulated by complex molecular mechanisms. Despite high levels of regulation, EGFR is frequently abnormally activated in epithelial tumors, and overexpression of EGFR has been correlated with poor clinical prognosis (2).

Crystallography studies of ErbB extracellular regions led to a significant advance in our knowledge of how EGFR dimerization and activation is promoted by growth factor binding (3). Dimerization is mediated by ligand-induced receptor–receptor interactions, and a "dimerization arm" in a cysteine-rich domain II at the dimer interface (4, 5) plays a critical role in this process. In the monomeric resting receptor (without ligand bound) this dimerization arm is buried intramolecularly by interaction with domain IV and thus appears to "autoinhibit" receptor dimerization (6). Activating ligands bridge two distinct binding sites on the receptor (in domains I and III) and induce domain rearrangement in the extracellular region of the receptor, leading to homo- and/or heterodimerization and *trans*-autophosphorylation of the intracellular domain of the receptor (7) (Fig. 1).

Characterization of this complex mechanism of receptor activation has triggered the development of various strategies to intervene in EGFR signaling, as reflected by two classes of anti-EGFR drugs that are currently used clinically: tyrosine kinase inhibitors (TKIs) and monoclonal antibodies (mAbs). TKIs represent small-molecule inhibitors that block EGFR-kinase activity by binding to the ATP-binding pocket, thereby abrogating downstream EGFR signaling. The effects of TKI seem to be primarily related to enzyme inhibition.

For mAbs, the mechanisms of action are more diverse and their relative contribution to antitumor activity is still being investigated. Most EGFR mAbs bind to the EGFR ligand-binding domain and thereby compete with the ligand for receptor binding. The chimeric EGFR mAb cetuximab, for example, interacts with EGFR domain III and occludes the ligand-binding region. Cetuximab has been described to prevent the receptor from adopting the extended conformation required for dimerization by causing steric clashes between the antibody's Fab domain and domain I of the receptor (8). mAb-mediated EGFR down-modulation is another mechanism that attenuates EGFR signaling. Antibody bivalency appeared to be an important prerequisite for this mechanism (9), although it was unclear how bivalent antibody binding of EGFR is compatible with EGFR inactivation, without *trans*-autophosphorylation by the kinase domains. Importantly, agonistic properties are frequently observed for mAbs directed against cell-surface receptors such as IGFR, C-Met, CD28, or Fas (10–12).

Our previous studies have shown that zalutumumab, a human IgG1κ EGFR antibody, potently inhibits tumor growth in xenograft models by engaging two mechanisms of action (13). First, EGFR signaling is blocked. This was observed as a reduction in receptor phosphorylation and is most effective at saturating antibody concentrations. Second, antitumor effects are mediated by Fc-mediated ADCC. In the present work, we studied the molecular mechanisms via which zalutumumab inhibits EGFR activation. First, we mapped the epitope of zalutumumab on EGFR. Then, we used Protein Tomography to visualize EGFR conformations in EGFR-overexpressing cells in its monomeric (resting) conformation, its EGF-stimulated conformation, and its zalutumumab-inhibited conformation. This technique allowed us to observe cell membrane-localized EGFR molecules

Author contributions: J.J.L.v.B., W.K.B., J.G.J.v.d.W., and P.W.H.I.P. designed research; J.J.L.v.B., A.B., A.v.E., M.P., and T.S.-M. performed research; J.J.L.v.B., W.K.B., A.B., A.v.E., M.J., T.V., J.G.J.v.d.W., and P.W.H.I.P. analyzed data; and J.J.L.v.B., W.K.B., A.B., J.G.J.v.d.W., and P.W.H.I.P. wrote the paper.

Conflict of interest statement: J.J.L.v.B., W.K.B., J.G.J.v.d.W., and P.W.H.I.P. are employees of Genmab. A.B., A.v.E., and M.J. are employees of Sidec. J.G.J.v.d.W. has substantive ownership of stock in Genmab BV.

This article is a PNAS Direct Submission.

Freely available online through the PNAS open access option.

¶To whom correspondence may be addressed. E-mail: ppa@genmab.com.

This article contains supporting information online at www.pnas.org/cgi/content/full/0709477105/DCSupplemental.

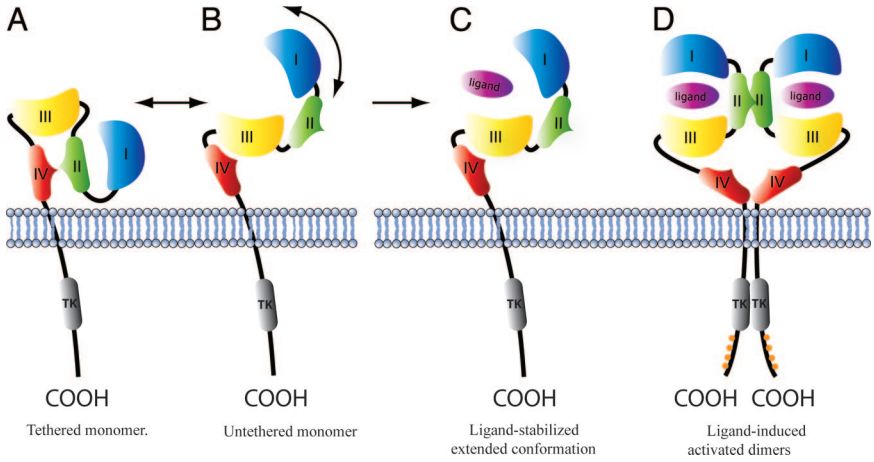

Fig. 1. Model for molecular mechanism of ligand-induced EGFR activation. EGFR domains are shown as a cartoon (domain I, blue; domain II, green; domain III, yellow; domain IV, red; intracellular tyrosine kinase domain, gray). (*A*) Most of the unliganded EGFR exists in an autoinhibited or tethered conformation, in which domains II and IV form an intramolecular interaction or tether. (*B*) In the remaining unliganded molecules, this tether is broken, and EGFR adopts a range of ''untethered'' conformations, some of which may be more extended. (*C*) Ligand binds preferentially to untethered molecules and interacts simultaneously with domains I and III, stabilizing the extended form in which domain II is exposed. (*D*) Dimerization is receptor-mediated and dominated by domain II interactions. In the dimer-complex, the intracellular kinase domains cross-phosphorylate residues in the C-terminal receptor tail. Adapted from ref. 8.

at a level of detail not previously obtainable; i.e., where separate protein domains could be discerned. Three-dimensional analyses of resting, EGF-bound, and zalutumumab-loaded EGFR provide a unique view of the mechanisms via which EGFR mAbs block EGFR activation and prevent EGFR tyrosine kinase activation.

Results

Bivalent Binding of Zalutumumab Without Activation of EGFR. Binding studies showed intact zalutumumab antibody to exhibit an ≈3-fold higher avidity for EGFR-expressing cells than its Fab fragment [EC_{50} intact IgG: 7 nM (C.I. 5–10); Fab: 19 nM (C.I. 15–24)]. This difference indicates bivalent zalutumumab binding to occur at the cell surface. Remarkably, this antibody-mediated cross-linking of EGFR did not result in EGFR activation, because we could not detect any induction of EGFR phosphorylation in starved A431 cells using an ELISA (data not shown). Instead, zalutumumab effectively blocked EGF-induced EGFR activation in a cell-based EGFR phosphorylation assay with an IC_{50} of ≈1.3 nM and was significantly more potent than Fab fragments (IC_{50} 10 nM) [supporting information (SI) Fig. S1]. In addition, A431 cell proliferation was more potently inhibited by intact zalutumumab antibody: IC_{50} 1.5 nM versus 13 nM for Fab fragments (Fig. S1). In the interpretation of the curve shift, it should be remembered that an intact IgG molecule may bind two EGFR molecules. However, because the maximum levels of inhibition were distinctly higher for intact zalutumumab, it became clear that bivalent binding is important for effective blockade of EGFR activation. To obtain a better understanding of the mechanisms underlying the enhancement of signaling inhibition by bivalent binding, we next analyzed the interaction at a molecular level.

Epitope Mapping. Previously, we found that zalutumumab inhibits EGFR ligand binding (13). This suggested that zalutumumab binds to an epitope located near the ligand-binding site. To investigate this further, we now evaluated zalutumumab binding to EGFR deletion-mutant EGFRvIII. EGFRvIII lacks amino acids 6–273, which comprise a deletion largely made up of domains I and II within the EGFR ectodomain. Zalutumumab binding to EGFRvIII was comparable with wild-type EGFR, indicating that its epitope is located in EGFR domain III or IV (Fig. S2). Cross-blocking with cetuximab, which also binds to domain III (8), indicated both antibodies to compete with each other for binding (data not shown; $n = 3$) by steric hindrance or allosteric changes in the epitope. However, mAb 528 (another EGFR antibody) blocked cetuximab but not zalutumumab binding to EGFR—suggesting overlapping but nonidentical epitopes. Because zalutumumab does not bind murine EGFR (13), 7 of 17 nonhomologous amino acid residues within domain III of human EGFR were changed to the corresponding murine amino acid residues by site-directed mutagenesis. These EGFR point-mutants were used to fine-map the epitope of zalutumumab. An additional point-mutant, K465E, which is known to affect cetuximab binding (14), was also included. The EGFR point-mutants were transiently expressed in HEK293 cells, and zalutumumab binding to point-mutants was evaluated as compared with wild-type human EGFR. EGFR point-mutants expression was verified by using a control mAb binding to EGFR domain II. Flow cytometric analyses identified four amino acids that were critical for zalutumumab binding: K465, M467, K443, and S418 (Fig. S2). Point mutations K465E and M467I exhibited the most striking effect, with no residual zalutumumab binding (Table 1).

Protein Tomography. Protein Tomography visualized conformations of individual EGFR proteins on cell surfaces at a resolution where separate domains could be identified. Native conformations of EGFR in resting (untreated) cells, activated (EGF-treated) cells, and antibody-inhibited (zalutumumab-treated)

Table 1. Zalutumumab binding to murine-human substituted EGFR point-mutants

Substitution	Reduction in zalutumumab binding, %
S418G	0
G471A	7
N473K	13
K443R	24
S468N	30
M467I	93
K465E	99

The reduction in zalutumumab binding is indicated as a percentage relative to wild-type EGFR. Data of a representative experiment are shown ($n = 2$).

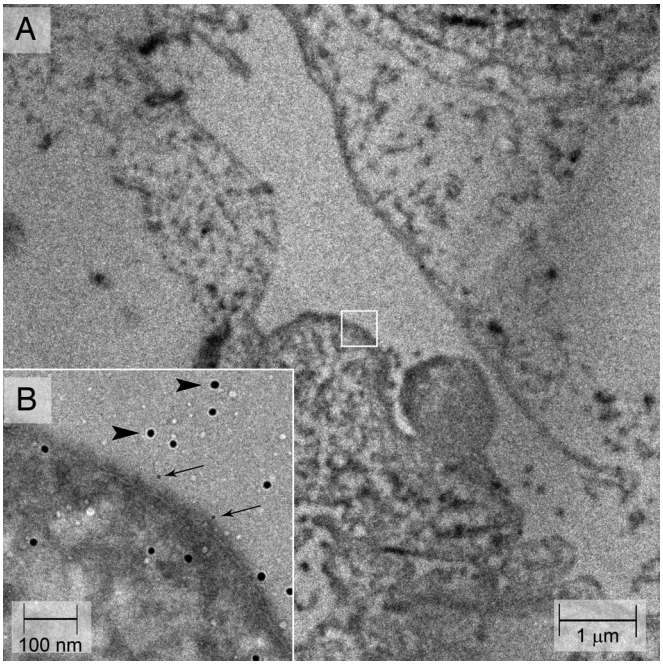

Fig. 2. Electron micrograph of A431 cell sections. (*A*) At ×2,300 magnification, where several cells can be seen, an area was chosen for Protein Tomography. (*B*) Inset showing a postimage of the final experimental area at ×20,000 magnification. Ten-nanometer colloidal gold particles (arrowheads), used for alignment of the tilt series, as well as 5-nm marker gold particles (arrows) bound to EGFR close to the plasma membrane of an A431 cell, can be seen in the micrograph.

cells could thus be compared to elucidate the underlying molecular mechanisms of activation and inhibition. The initial steps of Protein Tomography include localization of gold-conjugated detection antibodies (marker gold) (Fig. 2) and collection of tilt series. Tomograms were generated from 95 tilt series (17 of the untreated sample, 43 of the EGF-treated samples, and 35 of the zalutumumab-treated samples). Six tomograms were excluded from analyses because of empty marker gold particles (not coated or coated but not bound to primary antibody) or marker gold residing in complex interactions of connected proteins. Six tomograms of untreated EGFR, eight tomograms of EGF-bound EGFR, and six tomograms of zalutumumab-bound EGFR (four monovalently bound, two bivalently bound) were selected for further analyses. The Protein Tomography analysis included investigating the size and shape of tomograms and comparing them by superimposing existing crystal structures.

Conformations of Resting EGFR. Fig. 3 shows three tomograms of individual resting EGFR molecules on untreated cells. The plasma membrane appears as a void, leaving the transmembrane part of proteins visible as a thin stalk. A number of EGFR conformations can be seen. In the majority of the tomograms, domains I–IV are oriented essentially in one plane. Resting EGFR shows conformational flexibility in the ectodomain exhibiting both tethered ($n = 2$; Fig. 3*A*) and "pistol"-shaped ($n = 4$; Fig. 3 *B* and *C*) variations. To enable better understanding of these EGFR conformations, crystal structures of EGFR domains [Protein Data Bank (PDB) entries 1NQL (ectodomain; ref. 6) and 2GS7 (kinase domain; ref. 15)] were superimposed and compared. These results showed the tethered EGFR conformations revealed in the tomograms to be rather similar to conformations found in the ectodomain EGFR crystal structure. The pistol-shaped EGFR, however, had a slightly more open or extended conformation than observed in crystal structures; i.e., its tertiary structure appeared different with larger distances between domains I/II and domains III/IV (resembling a half-opened "jackknife"). To obtain an accurate fit between pistol-shaped EGFR and available x-ray structures, the tethered EGFR x-ray structure had to be opened; i.e., domains I/II moved further away from domains III/IV. Protein Tomography thus suggests that the general shape of monomeric, resting EGFR on cell surfaces is flexible and can exist in either tethered or half-extended conformation.

In addition, in some tomograms we observed an extra volume extending from domain I of EGFR (see, e.g., Fig. 3*b* and Fig. 5). EGFR on A431 cells is glycosylated, adding on 40 kDa to the 130 kDa of unglycosylated EGFR (16). There are two glycosylated sites located on domain I (17). Because Protein Tomography is unable to discriminate between protein and carbohydrates, it is likely that the extra volumes in the tomograms represent carbohydrate groups extending from domain I.

Conformation of EGF-Bound EGFR. Cells were incubated with a saturating concentration of EGF. EGF-bound receptors located at the cell membrane were measured by flow cytometry and found to number ≈80% of a control prepared at 4°C (Fig. S3). EGF-induced EGFR autophosphorylation was also verified by immunoblotting. Strong EGFR tyrosine phosphorylation was observed compared with cells incubated in culture medium only, thus indicating the presence of EGF-stimulated EGFR molecules (Fig. S3).

Fig. 4 shows a tomogram of EGF-bound EGFR. EGFR ectodomains were consistently observed as two ring-like structures with some flexibility at the interface between them. Superimposing the crystal structure of the EGFR homodimer complex of human EGF on extracellular domains I–III [PDB entry 1IVO (4)] showed that the activated EGFR molecules

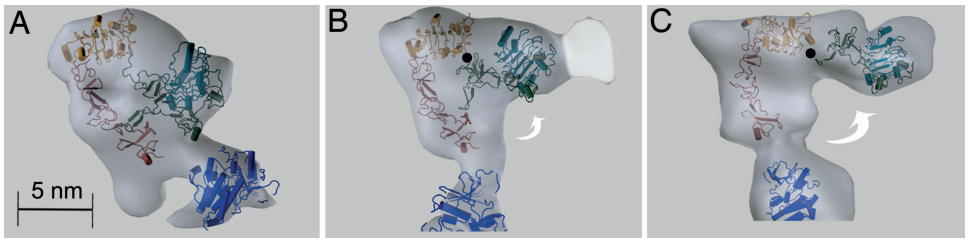

Fig. 3. Conformations of nonactivated EGFR. Shown are three of a total of six analyzed tomograms of individual cell membrane-expressed EGFR on untreated cells (*A–C*). Tomograms have been cropped to include EGFR only, leaving out marker golds and antibodies. The lipid bilayer of the protein complex is not visualized because of the staining method used. The ribbon diagrams of the EGFR crystal structures from PDB entries 1NQL (6) and 2GS7 (15) were superimposed into the tomograms. The ectodomain crystal structure is color-annotated (domain I, blue; domain II, green; domain III, yellow; domain IV, red). Rotational flexibility (as indicated by white arrows) of the rigid body containing EGFR domains I and II about the axis represented by a black circle (at the domain II/III junction) allows a better fit of all domains in the tomograms illustrating conformational flexibility within EGFR. An undefined volume is shown in white in *B* and likely represents carbohydrates extending from domain I. Tomograms are also available as interactive 3D files (Fig. S4) and as a movie (tomogram C) (Movie S1).

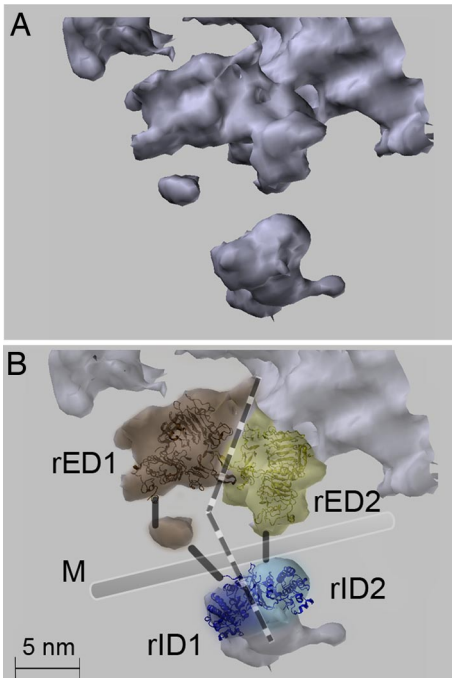

Fig. 4. Conformation of EGF-bound EGFR homodimer. (*A*) Tomogram of an EGF-bound EGFR homodimer identified on the cell membrane of A431 cells. The lipid bilayer is not visualized in a tomogram and appears as a void. (*B*) The crystal structure of the complex of human EGF and EGFR extracellular domains I–III [PDB entry 1IVO (4)] was superimposed into the receptor ectodomain in a ribbon diagram representation. The different receptors rED1 and rED2 are colored brown and yellow, respectively. A proposed position for the lipid bilayer is annotated as a shaded gray bar. The crystal structure of active EGFR kinase domain [PDB entry 2GS2 (15)] was superimposed into the intracellular domains rID1 and rID2 (blue) ($n = 8$). The model proposed here is consistent with ligand-stabilized domain II-mediated interactions. The intracellular domains in the complex are in close spatial proximity to each other and visible as a merged volume. This tomogram is also available as an interactive 3D file (Fig. S4).

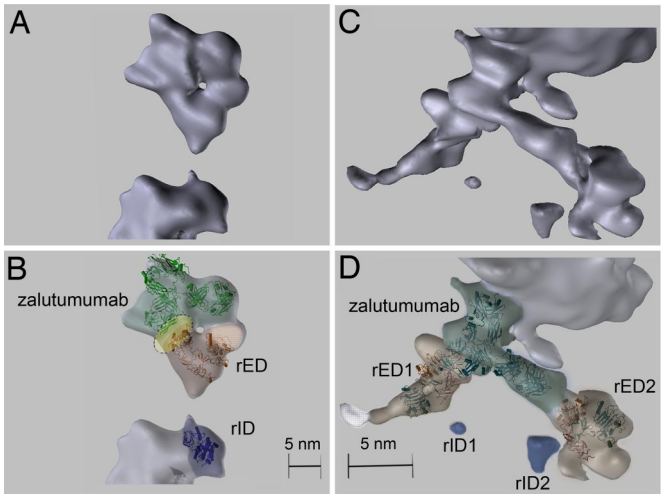

Fig. 5. Conformation of zalutumumab-bound EGFR. Shown are tomograms of zalutumumab-bound EGFR. In *B* and *D*, the tethered crystal structure of sEGFR (PDB entry 1NQL, shown as a ribbon representation) was superimposed into EGFR ectodomain tomograms. The crystal structure of human Ig 1 [PDB entries 1HZH (*A*) (33) and 1IGY (*B*) (34)] was superimposed into zalutumumab (green). (*A* and *B*) show a tomogram of a zalutumumab molecule monovalently bound to EGFR. The complex was marked by anti-EGFR-3.5 nm colloidal gold-conjugated protein A intracellular labeling only. The dotted line in *B* marks the zalutumumab docking site on EGFR. The EGFR ectodomain structure is condensed and resembles the tethered EGFR conformation, when zalutumumab is bound ($n = 4$). (*C* and *D*) show tomograms in which one zalutumumab antibody molecule binds two EGFR molecules. Zalutumumab binds one EGFR molecule with each of its Fab arms, spatially separating the two receptors ($n = 2$). The extra volume present on EGFR domain I (white) likely represents carbohydrate chains. Both tomograms are available as interactive 3D files (Fig. S4) and as movies (Movies S2 and S3).

display a tilted orientation in relation to each other, as well as an interface on domain II. In the tomogram, a small void was observed between domains III and IV that was likely caused by low electron density of this part of the receptor that could be visualized at higher contrast levels. Significantly, EGFR in resting, activated, and inhibited states was on several occasions positioned in parallel with the plasma membrane rather than occupying a vertical position. For all eight identified, cell-surface-localized EGF–EGFR protein structures, the intracellular kinase domains were observed in close proximity to each other (1–2 nm) and are mainly visible as a merged volume. For structural analyses, the crystal structure of the active EGFR kinase domain [PDB entry 2GS2 (15)] was superimposed on the intracellular domains. In our study, only EGF-bound EGFR dimers were identified ($n = 8$). Similar to our findings for monomeric resting EGFR, we also observed an extra volume extending from domain I on some of the activated EGFR structures.

Conformation of Zalutumumab-Bound EGFR. Cells were incubated with a zalutumumab concentration at its K_D to achieve ≈50% saturation of the cell-surface EGFR. Under these conditions, monovalent as well as bivalent zalutumumab binding could be anticipated. Zalutumumab saturation and inhibition of EGF-induced EGFR phosphorylation were verified and shown to be ≈50% and 45%, respectively (Fig. S3). Fig. 5 shows tomograms of zalutumumab-bound EGFR. In Fig. 5*A*, the zalutumumab structure can be recognized by the characteristic "Y"-shaped antibody, as previously observed by Sandin *et al.* (18), also using Protein Tomography analyses. Zalutumumab binds to the top of the receptor via one Fab arm and with the Fc domain directed away from the cell membrane (Fig. 5). The other Fab arm is found in close proximity to glycans on domain I. Condensed EGFR conformations were observed for all six zalutumumab–EGFR complexes compared with monomeric resting EGFR. Superimposing the tethered EGFR ectodomain crystal structure (PDB entry 1NQL) showed that the EGFR conformations seen in the tomograms closely resemble the crystal model. (Domains I–IV were correspondingly oriented in the same plane as observed for EGFR in untreated cells.) Superimposition data also revealed that the site of interaction between EGFR and zalutumumab Fab domains was located in EGFR domain III in all six identified zalutumumab–EGFR tomograms.

Complexes in which zalutumumab binds two EGFR molecules were also identified and analyzed ($n = 2$). As Fig. 5 *C* and *D* shows, zalutumumab binds one EGFR molecule with each Fab arm. In this complex, the antibody's Fc domain is also directed away from the cell membrane. Furthermore, just like monovalently bound EGFR, bivalently bound zalutumumab–EGFR complexes are condensed and resemble the crystal structure conformation of tethered EGFR (PDB entry 1NQL). In addition, the intracellular EGFR kinase domains were oriented relatively far from each other in the bivalently bound tomograms: 17–32 nm compared with 1–2 nm observed for EGF-bound EGFR dimers. No contact between the two kinase domains was observed. In summary, EGFR molecules are in a very compact conformation when bound to zalutumumab, and the conformational flexibility of EGFR ectodomain appears

minimal. Bivalent binding leads to considerable spatial separation of EGFR kinase domains.

Discussion

Zalutumumab binding to EGFR is sufficient to inhibit receptor activation. However, inhibition by the intact antibody is known to be more potent than that by Fab fragments and therefore bivalent binding has been postulated to play an important role in this inhibition (9). Previous studies by Fan *et al.* (9) highlighted the importance of anti-EGFR bivalency with respect to therapeutic efficacy. We have elucidated the binding target of the zalutumumab–EGFR interaction by fine-mapping the epitope using deletion mutant EGFRvIII and human-murine EGFR point-mutants, and further analyzed its structural consequences by Protein Tomography studies. We also studied the conformations of resting and ligand-activated EGFR to be able to compare receptor conformations in different states.

Protein Tomography data revealed that resting EGFR in its natural cellular environment is a flexible molecule. The tomograms shown represent "snapshots" of the various conformations that EGFR molecules may occupy in time. A number of conformations of the EGFR ectodomain on resting cells were observed, suggesting that it is able to switch between a tethered (autoinhibited) conformation and extended pistol-shaped conformations. This visualization of a flexible receptor located intact on the cell surface thus supports models suggested previously (4–6).

In the present study, only EGFR monomers were observed in untreated cells, in contrast to the inactive preformed EGFR dimers that have been described by others using different techniques (19, 20). In the tomograms of EGF-bound EGFR, the ectodomains were characterized as ring-like structures with an interaction interface between them. Superimposing the crystal structure of human EGF in complex with EGFR [PDB entry 1IVO (5)] gave an accurate fit for both the size and shape of the structures, and matched the model of "extended" EGFR dimer formation. The high consensus between the native ring-like structures demonstrated that EGF-bound EGFR possesses little flexibility, a parameter that cannot easily be deduced from crystal structures. In contrast, on the interfaces between the ring-like EGFR structures, some flexibility was observed. Furthermore, we observed the intracellular kinase domains to be in close proximity to one another for all identified EGF-bound receptors. This supports earlier reports that EGFR kinase activation depends on mutual allosteric interactions between EGFR kinase domains (15).

In contrast to the flexible conformations observed for monomeric, resting EGFR, zalutumumab-bound EGFR conformations were condensed and appeared to be locked in one specific conformation. Superimposing crystal structure (PDB entry 1NQL) into zalutumumab–EGFR indicated that the zalutumumab-binding site is located on EGFR domain III. Fine-mapping analyses confirmed that the binding epitope is situated on this domain. This mechanism resembles a mechanism earlier described for cetuximab (8). Binding of cetuximab may prevent EGFR from adopting the extended conformation by steric hindrance between the Fab arm and the N-terminal portion of domain I. Although crystallography analyses have suggested some conformational flexibility of cetuximab-bound EGFR, we have repeatedly observed only compact conformations for the zalutumumab-bound receptor.

In addition to monovalently bound EGFR molecules, we also saw that zalutumumab bound bivalently. Observations that intact zalutumumab was more potent than Fab fragments suggested that the mechanism of EGFR inhibition by intact antibodies is more complex. Like EGFR molecules in monovalently bound zalutumumab–EGFR complexes, EGFR molecules in bivalently bound complexes were only seen in compact conformations. Notably, there was no interaction observed between the two EGFR kinase domains in these complexes.

The distance between the kinase domains as interpreted from Protein Tomography data were ≈17–32 nm, and it seems that binding of zalutumumab to the EGFR ectodomains causes this spatial separation. Flexibility of IgG1 Fab domains is large (18, 21, 22), and the minimum distance between IgG Fab domains as observed in several nonliganded structures is 5.5–7.0 nm. If receptor monomers interacting with bivalent antibody could come in this close proximity, then this could possibly result in undesired receptor activation. Protein Tomography, however, allowed us to examine the structure of bivalent antibodies bound to receptors associated with the cell surface, revealing additional structural constraints. Significantly, we observed that under these conditions, bivalent antibody binding separates kinase domains sufficiently to impair efficient EGFR transphosphorylation. This observation explains the increased ability for receptor inactivation of bivalent antibody. This effect may further be augmented by the orientation of the EGFR molecules in the complex in which kinase domains are oriented away from each other. Indeed, our studies suggest that ligand-binding inhibition alone may not be sufficient for optimal EGFR signaling inhibition and that preventing kinase activation through antibody-mediated receptor cross-linking by restricting intermolecular flexibility, in addition, is essential. This notion is supported by the observations that kinase-stimulatory antibodies have been identified for various cell-surface receptors (10–12) and that both EGFR orientation and conformation in the dimer are critical for efficient kinase activation. It can be speculated that ligand-blocking antibodies that do allow dimerization of kinase domains following receptor cross-linking might be poor inhibitors of signaling or even display agonistic activity. By design, we excluded such antibodies in the screening assays used in the isolation of zalutumumab by selecting for antibodies that potently inhibited both EGFR-ligand binding and EGFR signaling (13).

mAb-induced spatial separation of EGFR kinase domains represents a mechanism of EGFR inhibition that may well explain the potency difference observed between whole antibody and Fab fragments, although it cannot be excluded that other mechanisms are involved. Stronger induction of EGFR degradation in endosomal compartments by the whole antibody may also be a factor, even though our previous experiments have suggested that induction of EGFR down-regulation is not a major mechanism of action for mAb 2F8 (13, 23).

In conclusion, visualizing EGFR conformations by Protein Tomography shows that antibody-mediated inhibition of EGFR activation by zalutumumab acts via two distinct mechanisms. (*i*) When zalutumumab binds to the EGF-binding site on domain III, it inhibits EGFR activation by restricting the molecule's conformational flexibility. This mechanism is primarily based on the monovalent interaction of the antibody Fab arm with the EGFR protein. (*ii*) When zalutumumab binds bivalently, EGFR forms specific antibody cross-linked, inactive EGFR dimers by spatial separation of two EGFR molecules. Because activation of cell signaling by (ligand-induced) dimerization of cell-surface receptors represents a general concept in cell biology, inhibition of receptor signaling by antibody-mediated spatial separation might therefore be applicable to other cell-surface receptors; e.g., ErbB family members. In summary, our study highlights how ligand blockade and kinase domain separation by a therapeutic mAb may cooperate to exert unique effects on EGFR structure resulting in optimal inhibition of a potent signaling molecule.

Materials and Methods

Cell Lines and Antibodies. A431 is a squamous carcinoma cell line from the German Collection of Microorganisms and Cell Cultures (Braunschweig, Germany; cell line number ACC 91) that overexpresses EGFR at levels in excess of 1×10^6 receptors per cell (24). Cells were cultured in RPMI medium 1640

(BioWhittaker) supplemented with 10% heat-inactivated calf serum (HyClone), 50 units/ml penicillin, and 50 μg/ml streptomycin. Zalutumumab (mAb 2F8, HuMax-EGFr), a human IgG1κ EGFR mAb, was generated as described in ref. 13.

Sample Preparation. Three A431 cell samples were prepared. The samples consisted of subconfluent monolayers of untreated A431 cells, 50 ng/ml EGF-treated cells (biotinylated EGF; Invitrogen), and 1 μg/ml zalutumumab-treated cells. EGF and zalutumumab-treated cells were incubated in at 37°C/5% CO_2 for 15 and 45 min, respectively. Thereafter, cells were fixed in 4% paraformaldehyde (PFA) for 10 min at room temperature. After 2 h, the cells were rinsed with 0.1 M phosphate buffer and postfixed in 2% PFA at 4°C until required for electron microscopy (EM).

Cryosectioning and Immunolabeling. EM preparation and immunolabeling of cryosections were performed essentially as described in ref. 25, based on the Tokuyasu method (26). Fifty- to 70-nm ultrathin cryosections were collected at −120°C. Sections were retrieved with a 1.15 M sucrose/2% methylcellulose pickup droplet and for Protein Tomography prepared parallel-bars grids (Agar Scientific). Ten-nanometer colloidal gold (GE Healthcare) was added to the grids and used for geometrical alignment of the tilt series.

Sections of untreated cells were labeled for EGFR by using affinity-purified polyclonal rabbit anti-EGFR antibodies (Cell Signaling Technology) specific for the EGFR intracellular domain. Antibodies were tested for specificity in immunohistochemistry, ELISA, and immunoblot. Sections of zalutumumab-treated cells were double-labeled for EGFR and zalutumumab. Anti-EGFR antibodies were detected with 3.5- or 5-nm colloidal gold-conjugated protein A (PAG) (Cell Microscopy Center, University Medical Centre Utrecht), and zalutumumab was detected with gold-conjugated (6 nm) goat anti-human IgG antibodies (Jackson ImmunoResearch Laboratories). Sections of biotinylated EGF-treated cells were single-labeled for EGF. Biotinylated EGF was detected by using rabbit anti-biotin antibodies (Dako), swine anti-rabbit antibodies (Rockland Immunochemicals), and 5-nm PAG (Cell Microscopy Center, University Medical Centre Utrecht). Briefly, nonspecific binding sites were blocked by incubating the sections in 0.15 M glycine in PBS followed by 1% BSA in PBS (incubation buffer). Sections were incubated with primary antibodies diluted 1:100 in incubation buffer for 1 h. Next, sections were washed in PBS and incubated with secondary marker in incubation buffer for 1 h, washed in PBS and in dH_2O. For double-labeling, a fixation step was performed before the second labeling was applied. Sections were contrasted with 2% uranyl acetate (UAc) in dH_2O, washed in dH_2O, embedded in 1% polyvinyl alcohol/0.3% UAc in dH_2O, and air-dried under cover.

EM and Protein Tomography. Protein Tomography was performed essentially as described in refs. 18, 27, and 28, using a Tecnai G2 Polara FEG transmission electron microscope (FEI Company) run at a 3.8-kV extraction voltage and a 300-kV acceleration voltage. Low-dose tilt series were recorded with a cooled slow-scan camera (2,048 × 2,048-pixel CCD chip, pixel size of 14 μm; Ultra Scan 1000; Gatan) using FEI automated tomography software. Tilt series of micrographs were recorded at 1° or 2° tilt intervals in the range ±60°, magnification ×20,000, postmagnification ×1.2, and final pixel size 5.73 Å. A postexperimental high-dose, large under-focus micrograph was recorded after each tilt series. Geometrical refinement was performed with gold markers (average alignment error for the tilt series was 6.9 Å). Density refinement was done with the COMET program (29–31) resulting in tomograms (3D density maps).The tomograms were visualized by using volume rendering in Sidec's in-house software Ethane. To superimpose crystal structures into tomograms, tomogram iso-surface representations were rendered by using Visual Molecular Dynamics visualization software (32), and the best fit was determined by visual inspection.

See *SI Materials and Methods* for additional details.

ACKNOWLEDGMENTS. We thank Dr. George Posthuma for preparation of cryosections for 3D-EM and Dr. Joost Bakker and Dr. Andreas Namslauer for help with the images.

1. Yarden Y, Sliwkowski MX (2001) Untangling the ErbB signalling network. *Nat Rev Mol Cell Biol* 2:127–137.
2. Gullick WJ (1991) Prevalence of aberrant expression of the epidermal growth factor receptor in human cancers. *Br Med Bull* 47:87–98.
3. Burgess AW, *et al.* (2003) An open-and-shut case? Recent insights into the activation of EGF/ErbB receptors. *Mol Cell* 12:541–552.
4. Ogiso H, *et al.* (2002) Crystal structure of the complex of human epidermal growth factor and receptor extracellular domains. *Cell* 110:775–787.
5. Garrett TP, *et al.* (2002) Crystal structure of a truncated epidermal growth factor receptor extracellular domain bound to transforming growth factor α. *Cell* 110:763–773.
6. Ferguson KM, *et al.* (2003) EGF activates its receptor by removing interactions that autoinhibit ectodomain dimerization. *Mol Cell* 11:507–517.
7. Schlessinger J (2000) Cell signaling by receptor tyrosine kinases. *Cell* 103:211–225.
8. Li S, *et al.* (2005) Structural basis for inhibition of the epidermal growth factor receptor by cetuximab. *Cancer Cell* 7:301–311.
9. Fan Z, Lu Y, Wu X, Mendelsohn J (1994) Antibody-induced epidermal growth factor receptor dimerization mediates inhibition of autocrine proliferation of A431 squamous carcinoma cells. *J Biol Chem* 269:27595–27602.
10. Prat M, Crepaldi T, Pennacchietti S, Bussolino F, Comoglio PM (1998) Agonistic monoclonal antibodies against the Met receptor dissect the biological responses to HGF. *J Cell Sci* 111:237–247.
11. Luhder F, *et al.* (2003) Topological requirements and signaling properties of T cell-activating, anti-CD28 antibody superagonists. *J Exp Med* 197:955–966.
12. Kahn CR, Baird KL, Jarrett DB, Flier JS (1978) Direct demonstration that receptor crosslinking or aggregation is important in insulin action. *Proc Natl Acad Sci USA* 75:4209–4213.
13. Bleeker WK, *et al.* (2004) Dual mode of action of a human anti-epidermal growth factor receptor monoclonal antibody for cancer therapy. *J Immunol* 173:4699–4707.
14. Chao G, Cochran JR, Wittrup KD (2004) Fine epitope mapping of anti-epidermal growth factor receptor antibodies through random mutagenesis and yeast surface display. *J Mol Biol* 342:539–550.
15. Zhang X, Gureasko J, Shen K, Cole PA, Kuriyan J (2006) An allosteric mechanism for activation of the kinase domain of epidermal growth factor receptor. *Cell* 125:1137–1149.
16. Zhen Y, Caprioli RM, Staros JV (2003) Characterization of glycosylation sites of the epidermal growth factor receptor. *Biochemistry* 42:5478–5492.
17. Wu SL, *et al.* (2006) Dynamic profiling of the post-translational modifications and interaction partners of epidermal growth factor receptor signaling after stimulation by epidermal growth factor using Extended Range Proteomic Analysis (ERPA). *Mol Cell Proteomics* 5:1610–1627.
18. Sandin S, Ofverstedt LG, Wikstrom AC, Wrange O, Skoglund U (2004) Structure and flexibility of individual immunoglobulin G molecules in solution. *Structure* 12:409–415.
19. Yu X, Sharma KD, Takahashi T, Iwamoto R, Mekada E (2002) Ligand-independent dimer formation of epidermal growth factor receptor (EGFR) is a step separable from ligand-induced EGFR signaling. *Mol Biol Cell* 13:2547–2557.
20. Martin-Fernandez M, Clarke DT, Tobin MJ, Jones SV, Jones GR (2002) Preformed oligomeric epidermal growth factor receptors undergo an ectodomain structure change during signaling. *Biophys J* 82:2415–2427.
21. Bongini L, *et al.* (2007) A dynamical study of antibody-antigen encounter reactions. *Phys Biol* 4:172–180.
22. Saphire EO, *et al.* (2002) Contrasting IgG structures reveal extreme asymmetry and flexibility. *J Mol Biol* 319:9–18.
23. Lammerts van Bueren JJ, *et al.* (2006) Effect of target dynamics on pharmacokinetics of a novel therapeutic antibody against the epidermal growth factor receptor: Implications for the mechanisms of action. *Cancer Res* 66:7630–7638.
24. Kwok TT, Sutherland RM (1991) Differences in EGF related radiosensitisation of human squamous carcinoma cells with high and low numbers of EGF receptors. *Br J Cancer* 64:251–254.
25. Raposo G, Kleijmeer MJ, Posthuma GP, Slot JW, Geuze HJ (1997) Immunogold labeling of ultrathin cryosections: Application in immunology. *Handbook of Experimental Immunology*, eds Herzenberg LA, Weir D, Blackwell C (Blackwell Science, Cambridge, UK), 5th Ed, Vol 4, pp 1–11.
26. Tokuyasu KT (1973) A technique for ultracryotomy of cell suspensions and tissues. *J Cell Biol* 57:551–565.
27. Bongini L, *et al.* (2004) Freezing immunoglobulins to see them move. *Proc Natl Acad Sci USA* 101:6466–6471.
28. Miralles F, *et al.* (2000) Electron tomography reveals posttranscriptional binding of pre-mRNPs to specific fibers in the nucleoplasm. *J Cell Biol* 148:271–282.
29. Skoglund U, Ofverstedt LG, Burnett RM, Bricogne G (1996) Maximum-entropy three-dimensional reconstruction with deconvolution of the contrast transfer function: A test application with adenovirus. *J Struct Biol* 117:173–188.
30. Fanelli D, Öktem O (2008) Electron tomography: A short overview with an emphasis on the absorption potential model for the forward problem. *Inverse Problems* 24, in press.
31. Rullgard H, Oktem O, Skoglund U (2007) A component-wise iterated relative entropy regularization method with updated prior and regularization parameter. *Inverse Problems* 23:1–19.
32. Humphrey W, Dalke A, Schulten K (1996) VMD: Visual molecular dynamics. *J Mol Graphics* 14:33–38, 27–28.
33. Harris LJ, Skaletsky E, McPherson A (1998) Crystallographic structure of an intact IgG1 monoclonal antibody. *J Mol Biol* 275:861–872.
34. Saphire EO, *et al.* (2001) Crystal structure of a neutralizing human IGG against HIV-1: A template for vaccine design. *Science* 293:1155–1159.